https://ntrs.nasa.gov/search.jsp?R=19660005764 2018-07-23T23:22:19+00:00Z

SOME INTENSITY MEASUREMENTS IN THE VACUUM ULTRAVIOLET

By

K. Watanabe, F. M. Matsunaga, and R. S. Jackson

Department of Physics

Prepared under Grant No. NsG-328

by the UNIVERSITY OF HAWAII, Honolulu, Hawaii

for

NATIONAL AERONAUTICS AND SPACE ADMINISTRATION

JUNE 1964

[redacted]

TABLE OF CONTENTS

ABSTRACT		iii
I	INTRODUCTION	1
	1. General	1
	2. Definitions	2
II	EXPERIMENTAL	5
	1. Apparatus	5
	2. Thermocouple Calibration	6
	3. Photoionization Measurements	9
	4. Photoelectric Measurements	13
III	PHOTOELECTRIC YIELD OF SOME METALS	16
	1. Photoelectric Yield of Untreated Samples	16
	2. Photoelectric Yield of Heat Treated Samples	20
	3. Photoelectric Yield of Gold Black	25
IV	PHOTOIONIZATION COEFFICIENT OF XENON	27
	1. Absorption Coefficient	27
	2. Photoionization Yield	31
V	PHOTOIONIZATION YIELD OF NITRIC OXIDE	35
VI	CONCLUSIONS	44
ACKNOWLEDGMENTS		46
REFERENCES		47
APPENDIX I		49
	Photoelectric Yields of Some Metals and Semiconductors	
APPENDIX II		56
	Absorption Coefficient and Photoionization Yield of Xenon	

ABSTRACT

15053

Photoelectric yields of twenty-three untreated metals, including gold black, and four semiconductors were measured in the region 900-2000 Å by means of a calibrated thermocouple. The yield curves showed no structure and in general confirmed previous results for several metals. The yields were usually reproducible in the region 900-1300 Å but less reproducible in the region 1300-2000 Å. Results for several heat-treated samples also confirmed previous data.

The photoionization yield of xenon as determined by a thermocouple was found to be unity in the spectral region 850-1022 Å which includes a number of broad preionized lines. Measurements were made at 230 wavelengths.

The photoionization yield of nitric oxide was determined at 470 wavelengths in the region 850-1345 Å with improved resolution. At Lyman alpha the yield was found to be 78 ± 5% in agreement with the previous recommended value of 81%.

Author

I. INTRODUCTION

1. General

Research in vacuum ultraviolet (vuv) physics has expanded rapidly during the past decade and significant advances have been made in the development of detectors, light sources, vacuum equipment, and optical instruments. However, techniques for absolute intensity measurement have improved slowly despite their need in the study of solar and other radiation sources, photochemistry, solid state physics, and plasma physics.

The measurement of absolute intensity is usually regarded as an inconvenient or tedious task, and most investigators have relied on "secondary standards" based on a few thermocouple measurements.[1-3] However, indirect comparisons under dissimilar conditions often lead to inconsistent results. For example, the quantum efficiency curve of a fresh coating of sodium salicylate is nearly flat,[2,4-6] but its shape changes gradually in vacuum. Hence, this phosphor is not a suitable material for a secondary standard. A recent report[7] shows that the photoelectric yield of nickel and lead sulfide in the vuv region may vary as much as an order of magnitude by changing the vacuum condition. If such a change is typical, one may question the reliability of a windowless photoelectric detector placed on a satellite for continuous observation.

Absolute intensities of vuv radiation have been measured by several methods. Packer and Lock[1] used a thermocouple at

the exit slit of a monochromator to make the first intensity measurement of dispersed vuv radiation. Several other investigators[2,3,5,7,8] have used thermocouples in a similar manner. For the region below 1022 Å, photoionization of rare gases provides a very convenient method for absolute intensity measurement. Watanabe and Marmo[9] have briefly reported that xenon has a quantum yield of unity (within about ± 10 %) in the region 850-1020 Å. Recently, Samson[6] reported that neon, argon, krypton, and xenon have the same relative quantum yield (± 5 %) at many wavelengths even in the autoionized lines of krypton. Thus it is extremely improbable that the photoionization yield of these gases is other than unity. In the soft X-ray region counting techniques[10] appear to be reliable. References to other methods are given in a paper by Hinnov and Hoffmann[11] who report on a still another method.

The present report describes our attempts to improve and extend our previous intensity measurements. It includes (a) the calibration of a thermocouple, (b) photoelectric yield of some metals and semiconductors, (c) photoionization yield of xenon at many wavelengths in the region 850-1022 Å which includes the preionized lines, and (d) photoionization coefficient of nitric oxide at many wavelengths in the region 850-1340 Å with improved resolution.

2. Definitions

a. Yield

The photoionization yield Y_i of a given gas for a

given photon energy is defined by the ratio of the number of primary ion pairs formed per second to the number of photons absorbed per second by the gas in an ion chamber. For molecules this yield is usually less than unity and may be as low as 10^{-4} especially near the ionization threshold. For atoms such as the rare gases and alkali metal vapor the yield can be unity, at least at wavelengths not coinciding with discrete energy levels.

The photoelectric yield Y_e of a solid may be defined by the ratio of the number of electrons emitted per second to the number of photons absorbed per second. Often the photoelectric yield Y_e' is defined by the ratio of the number of electrons emitted per second to the number of incident photons per second. If the incident photons are either absorbed or reflected by the solid, the two definitions are related by the equation

$$Y_e' = (1-R)Y_e \qquad (1)$$

where R = reflectance of the solid. In the vuv region R is small (order of 0.1) for most solids. For example, aluminum coating has been used most commonly for reflection grating in the vuv region, but Haas and Tousey[12] report that "At 2200 Å aluminum mirror shows very little reflectance decrease over a period of several years. At 900 Å, however, aluminum coating when just out of the evaporator reflects 20 %, but after a few days only 10 %." In the present study most of the metals were in the form of "untreated" metal strips, and the second

definition of yield Y_e' was used. Our main purpose was to first study the reproducibility of yield data for such untreated metals before investigating evaporated thin films.

b. Absorption and Photoionization Cross Sections

The total absorption coefficient k in cm^{-1} is defined by the equation,

$$I = I_o \exp(-kx) \tag{2}$$

where I_o is the incident and I the transmitted intensity of monochromatic light and x in cm is the layer thickness of gas reduced to $0^\circ C$ and 1 atm pressure.

The total absorption cross section σ in cm^2 is defined by the equation

$$\sigma = k/n \tag{3}$$

where n is Loschmidt's number (2.69×10^{19} particles per cm^3).

The photoionization coefficient k_i is defined by the equation,

$$k_i = Y_i k \tag{4}$$

where Y_i was defined in the preceding section. Similarly the photoionization cross section σ_i is defined by the equation,

$$\sigma_i = Y_i \sigma \tag{5}$$

II. EXPERIMENTAL

1. Apparatus

Two 1-meter, normal incidence, vacuum monochromators of the radius-mount type were used in the present study. Monochromator A which was described previously[13] provided a resolution of 0.2 Å when used with a platinized[14] grating having 1200 lines per mm and slits of 17 micron width. Four entrance and four exit slits were mounted on vertical circular plates which could be rotated in their planes. Monochromator B had a platinized grating with 600 lines per mm and a set of three slits which could be moved horizontally by a push-pull shaft. This type of slit motion was found to be suitable for thermocouple measurements, and the slit mount was modified to accommodate the thermocouple. Monochromator A was used for measurements of absorption cross section and photoionization of xenon and nitric oxide while the second monochromator was used primarily for photoelectric emission studies of solids with the thermocouple.

Windowless hydrogen discharge tubes were used for light source. They were usually operated at 0.35 or 0.40 amp dc with about 700 V across the tube.

Most of the experimental methods and procedures used were described previously.[8,9,13] In the following sections we limit the description to thermocouple calibration and quantum yield measurements.

2. Thermocouple Calibration

A compensated, windowless Reeder thermocouple type RUV-5 with a detector area 1 x 3 mm was used in the present study. The thermocouple response was amplified by a Beckman Model 14 breaker amplifier and traced by a Speedomax recorder. The amplifier provided test voltages of 0.1, 0.3, 1 and 3 μv which were used as references but corrections up to 3 % were required to normalize them to the 1 μv deflection.

The thermocouple sensitivity in air was measured with a standard lamp (C-980) from the National Bureau of Standards according to the recommended procedure. In order to obtain consistent results, a slit had to be attached to the thermocouple so that only the detector surface (gold black deposit) was illuminated. The sensitivity of the detector element was found to be the same for several slit widths from 0.5 to 0.9 mm. A slit of dimensions 0.519 x 2.60 mm was finally selected so that, when used in the monochromator, the light beam would always strike the detector surface even when the beam direction is changed by moving the grating. The mean thermocouple sensitivity in air was 0.306 microvolt per microwatt.

To check our calibration method, the sensitivity of an Eppley thermopile was measured by the same method. Our result was within 1 % of the value determined by the Eppley Laboratory.

The thermocouple was placed in the exit slit housing of monochromator-B as shown in Fig. 1, and its sensitivity in vacuum was measured in the following manner. The thermocouple

was attached to a slit mount which can slide in a horizontal direction. The thermocouple leads were passed through the wall of the vacuum chamber and soldered with the recommended solder directly to the input cable of the breaker amplifier. This arrangement eliminated the use of feed throughs which proved to be sources of erratic voltages. A glass window at the opposite end of the monochromator permitted a lamp to illuminate the thermocouple. The vacuum-to-air response ratio was obtained by measuring the thermocouple response first with several chamber pressures in the range from 10^{-4} to 5×10^{-4} mm Hg of H_2 gas and then with the chamber filled with air at 1 atm. This ratio (22.0) was nearly constant for the range of chamber pressures used under operating conditions. The vacuum sensitivity of the thermocouple for most of the present study was 6.73 μv/μw, which compares favorably with those reported by others: 1.6 by Packer and Lock,[1] 1.3 by Watanabe and Inn,[2] 1.05 by Wainfan *et al.*,[3] and 0.482 by Smith.[5]

There are at least two possible sources of systematic errors in the present calibration: (a) the assumption that the "blackness" of the thermocouple is the same in the vuv and in the light of the standard lamp; (b) loss of energy to photoelectrons emitted from the detector surface.

Gold black may be truly black to vuv radiation, according to Samson,[6] because most materials have low reflectance in the vuv. In fact, Smith's[5] experimental value of the reflectance of gold black is about 0.3 % in the photon energy range from 7 to 14 eV. Lee and Seliger[15] caution that although

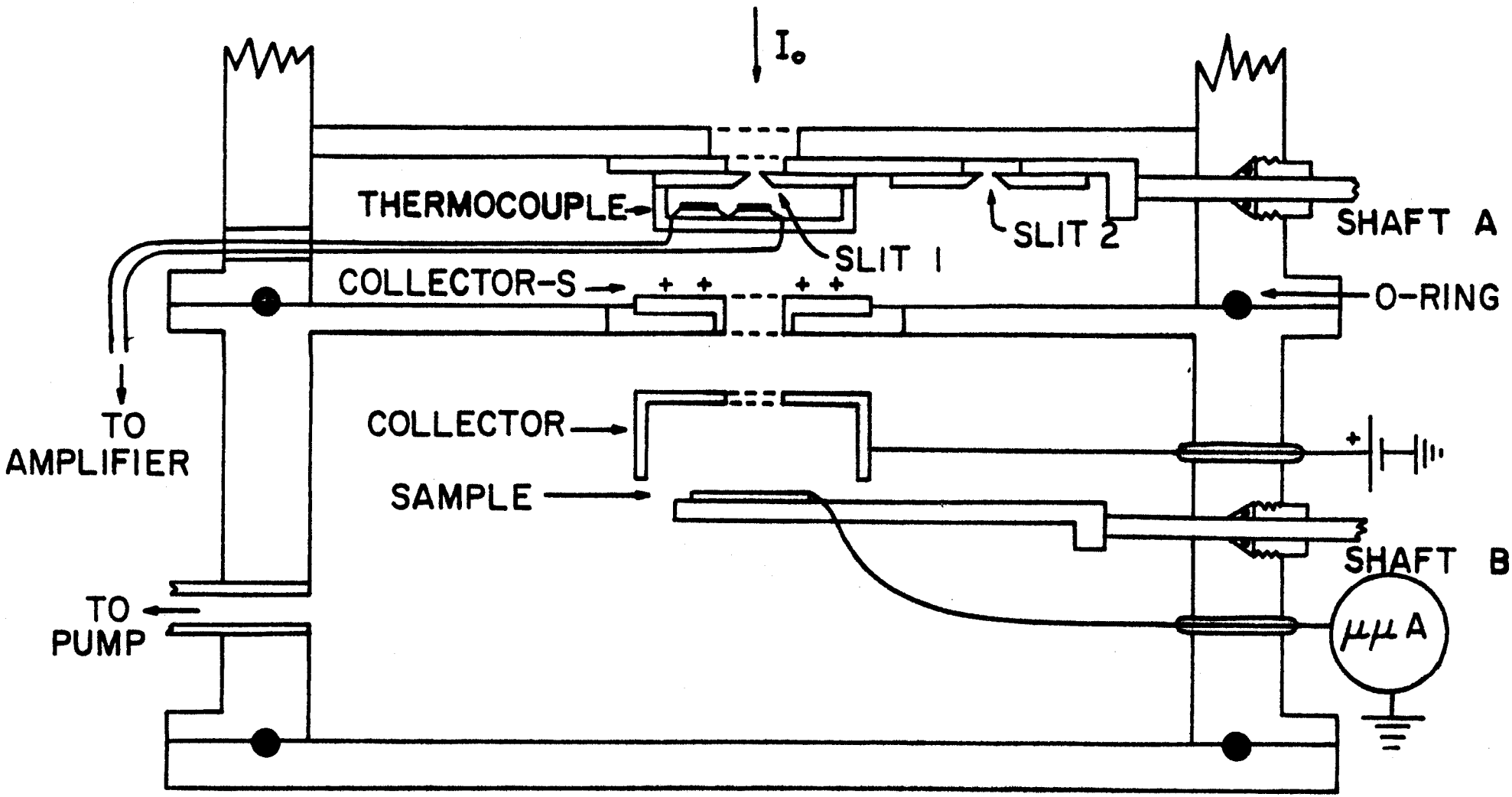

Figure 1. Schematic diagram of photo-cell with themocouple

deposits of gold black can be highly non-selective in the visible and near IR regions as shown by Harris et al,[16] the same may not be the case for thin evaporated films used in "fast" thermocouples. Our Reeder thermocouple appears to be the former type on the basis of some results to be discussed later.

The emission of photoelectrons from the detector surface of our thermocouple was measured and is described in the Part III of this report. Here, we mention that the error introduced by neglecting energy loss due to photoemission appears to be small.

3. Photoionization Measurements

The photoionization of nitric oxide and xenon was studied with windowless ion chambers in a manner similar to that described for the case of oxygen.[9] However, improvements were made by using (a) more efficient ion chambers, (b) a more reliable method of pressure measurement, and (c) a calibrated platinum photoelectric detector in place of a phosphor-coated photomultiplier.

The ion chamber as used at first had a cell length of 13.6 cm and two parallel-plate electrodes extending over nearly the length of the cell. This arrangement required a correction for some ions lost to the exit slit mount, especially for relatively high gas pressures ($\sim$0.5 mm Hg). Hence, the cell was modified by (a) increasing the cell length to 27.1 cm and (b) electrically insulating the slit jaws from the slit mount and connecting them to the positive plate.

Fig. 2 is a schematic diagram of the ion chamber which is similar to that used by Samson.[6] Consistency in the results obtained with different pressures indicated that practically all ions were collected by the negative plate and measured by the micro-microammeter.

The calibrated photoelectric detector (labelled P in Fig. 2) consisted of a cylindrical collector and a flat piece of platinum cathode both imbedded in a piece of teflon. The detector could be moved in and out of the light path by a push-pull shaft. The collector and the platinum cathode were connected to the two parallel plates as shown in Fig. 2. The detector was calibrated against the thermocouple several times during the study and found to give reproducible results. Voltages used across the plates were in the range 10-20 V which was in the plateau of the voltage-current curve.

During measurements of ion current, the gas flowed from the gas-handling system into the ion chamber and then out of the exit slit (width 17 or 40 microns). The flow rate of gas into the ion chamber was controlled by a needle valve with a micrometer handle. A liter of reagent grade xenon (Airco) at 1 atm was sufficient for the absorption and photoionization measurements in the region 850-1025 Å, but nearly two liters of nitric oxide was required to cover a more extensive region 850-1350 Å.

Pressures from 0.01 to 0.4 mm Hg in the ion chambers were measured with a Consolidated micromanometer which was connected directly to the ion chamber as indicated in Fig. 2. As

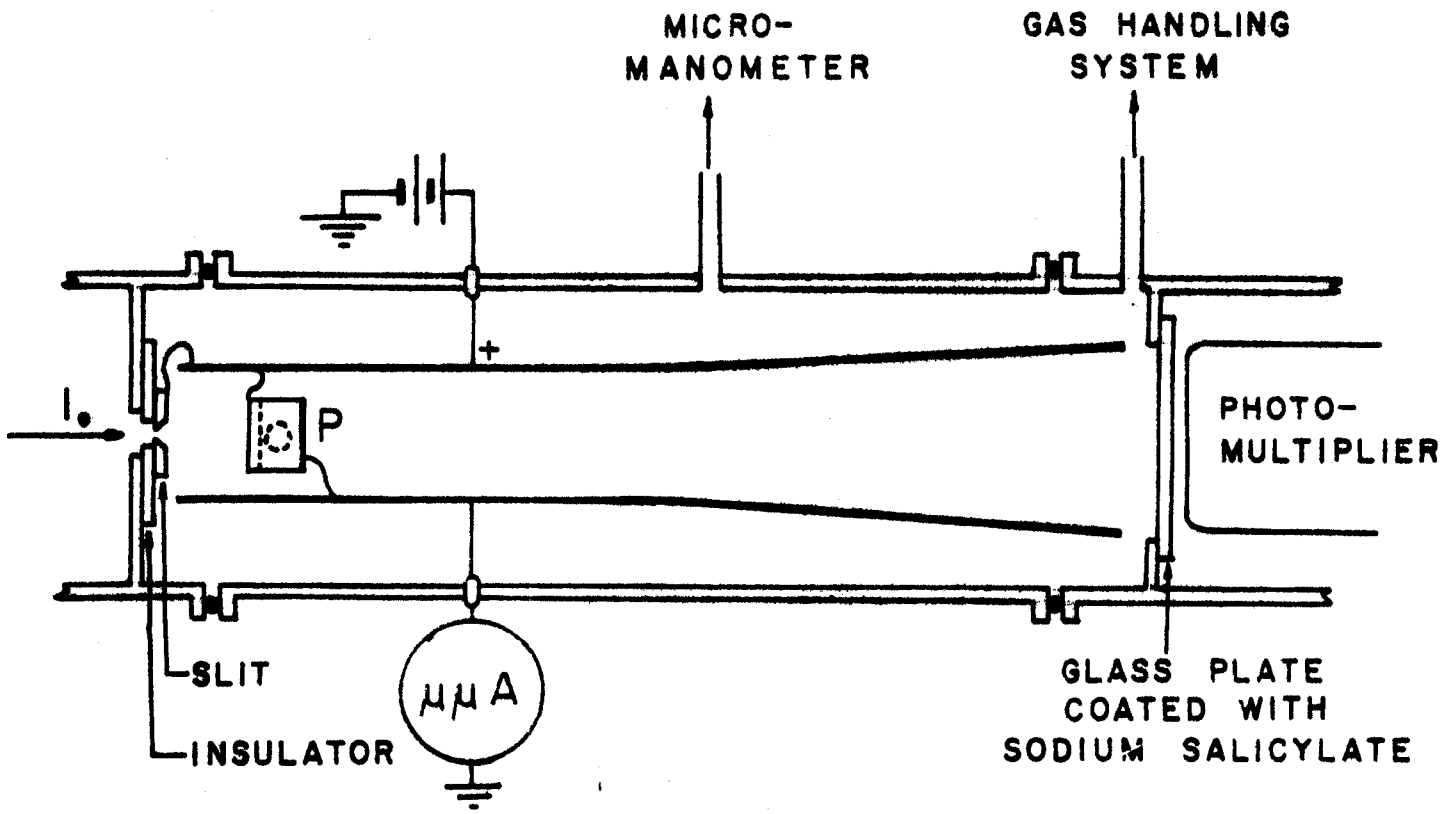

Figure 2. Schematic diagram of free-flow ion chamber

described previously,[9] it is possible to determine the effective pressure of a gas in a windowless cell by inserting accurately known absorption coefficients and measured values of I/I_o into equation (2). Using this method a curve (straight line in log-log scale) for dial reading vs pressure was obtained with O_2 gas ($k = 394\ cm^{-1}$ at 1435.3 Å) and CO_2 ($k = 4900\ cm^{-1}$ at 1121.25 Å). Next, the windowless cell was replaced by a cell with windows, and a curve for dial reading vs pressure as measured directly with a McLeod gauge was obtained. The two curves overlapped within experimental error over the pressure range 5 to 550 microns. Hence, the pressure gradient in the ion chamber was apparently very small.

A set of data consisted of the following recorder traces: (1) photoemission current of the platinum detector at the beginning, (2) three to five runs of photoionization current using different gas pressures, (3) another run of photoemission current of platinum. The scanning speed was usually 2.5 Å/min and the spectral range covered per run was about 50 Å.

The photoionization yield of the gas was computed from the photoelectric yield of platinum and the ratio of the ion current to the photoelectric current. If the absorption of light by the gas was incomplete, the fraction of radiation absorbed was computed with the previously measured absorption coefficients.

4. Photoelectric Measurement

Absolute photoelectric yields of some solids were determined by using the arrangement shown in Fig. 1, which shows a typical sample chamber mounted behind the slit housing. The collector was a brass cup with an aperture for the incident light. It was connected to the positive terminal of a battery power supply via a feed through. A second collector (collector-S in Fig. 1) was placed closer to the exit slit to collect electrons emitted from the slit jaws. In some sample chambers this collector was not necessary. Emission current from a sample was measured with a Beckman micro-microammeter, Model V. For survey studies four samples were mounted on a push-pull shaft (e.g. shaft B in Fig. 1), and measurements were made successively without breaking the vacuum. A collector voltage of less than 5 V gave saturation current, but usually 10 or 15 V was used.

Metal sheets were obtained from A. D. Mackay, Incorporated, and studied in most cases without heat treatment. These "untreated" samples were, however, cleaned with benzene or acetone before placing them in the sample chamber. A few samples such as silver were polished to remove apparent oxide layers.

Several metals were studied after heat treatment at temperatures up to 1500°C in vacuum. In this case, a somewhat different sample chamber was used. The sample was rigidly clamped on a support, a heavy current was passed through the sample (about 0.1 mm thick) for a definite time,

and the temperature was estimated with an optical pyrometer through a glass window located behind the sample. All measurements were made after the heat-treated sample had approached room temperature.

The photoelectric yield of gold black was measured in a unique manner. First, the thermocouple was used to measure the spectral intensity in the region 900-1400 Å. Next, the two electrical leads of the thermocouple were joined and connected to the positive terminal of a battery power supply via a one-megohm resistor. The negative terminal of the battery was connected to the input of a micro-microammeter. The thermocouple mount (see Fig. 1), which almost completely enclosed the gold black detector element, was used as a collector at ground potential. Next, to measure the photoemission current, a negative voltage was applied to the gold black element. The leakage current from the thermocouple elements to ground was several times the photoelectric current; however, the former was sufficiently constant to permit subtraction. The saturation current was obtained with minus 7 V on the gold black element. Finally, the thermocouple was again used to measure the spectral intensity.

A set of data usually consisted of (a) two scans of the H_2 spectrum with the thermocouple, (b) two scans of photoelectric current, (c) two final scans with the thermocouple. Since photoelectric yield curves of metals and semiconductors show no fine structure in the vuv region, a spectral band width of about 9 Å was considered as quite adequate. The

traces of the H_2 spectrum obtained in the present work showed more structure than the trace presented in reference 2 where a band width of 18 Å was used.

III. PHOTOELECTRIC YIELD OF SOME METALS

Photoelectric effect in metals has been studied to a very limited extent in the vuv region as one may infer from a review by Weissler.[17] Most of the published results for this region are due to Wainfan, Walker, Rustgi, and Weissler.[3,18,19] They used photon energies from 10 to 26 eV to study the following metals: Pt and Ta,[3] Ag, Au, Cu, Mo, Ni, Pd, and W,[18] and Al, Bi, In, and Sn.[19] Hinteregger reported on Be,[20] Ni, Pt, and W.[21] Published data for the region 6-12 eV is very meager.

The present measurements were made in the spectral region 900-2000 Å or about 13-6 eV. For convenience of discussion, the results are described in the following three sections.

1. Photoelectric Yield of Untreated Samples

The reproducibility of the photoelectric yield of a sheet of platinum (sample A) was studied by taking measurements on nine days during a period of eighteen days. After each of the nine measurements, the sample was exposed to air for about an hour; otherwise, it was kept in vacuum of 10^{-4} - 10^{-5} mm Hg (oil diffusion pump) or about 10^{-2} mm Hg (mechanical pump). The yield for the region 900-1350 Å was quite reproducible (± 10 % or less); however, the yield at longer wavelengths increased gradually during the period and at 1600 Å the yield increased by a factor of 2. Similar results were obtained for thin sheets of gold and palladium during a period of about two weeks. Thus, it appears that we cannot rely on the reproducibility of photoelectric yield of untreated samples in the

spectral region above about 1300 Å.

The absolute photoelectric yield differs somewhat for samples obtained from different sources. The results for three samples, A, B, and C are tabulated in Table I. The yields for sample A are considerably higher than those for sample C for the region 920-1300 Å but are lower at longer wavelengths. In Fig. 3, data points denoted by crosses and solid circles are for samples B and C, respectively. The yield at 1608 Å for sample C is about three times that of sample B, but the difference is comparatively small in the shorter wavelength region. Fig. 3 includes the yield curve of untreated platinum obtained by Wainfan *et al.*[3] and by Metzger and Cook.[22]

The reliability of our experimental method was checked by measuring the photoelectric yield of a Pt sample by comparison with the photoionization of xenon gas (see Part IV). In Fig. 3, solid circles are data points obtained by using the thermocouple method and open circles by the xenon method. The agreement is satisfactory in the overlapping region 920-1020 Å. Wainfan *et al.*[3] used the thermocouple method, while Metzger and Cook[22] used the second method.

Photoelectric yields of the following untreated metals and semiconductors are tabulated in Appendix I: aluminum, beryllium, cadmium, cobalt, copper, gold, indium, iron, lead, magnesium, molybdenum, nickel, niobium, palladium, platinum, silver (polished), tantalum, thorium, tin, titanium, tungsten, vanadium, zinc, zirconium, gallium-antimonide, germanium,

Table I Photoelectric Yield of Platinum in Percent

Columns A, B and C give the yields of three different samples obtained by using a thermocouple as standard. Column B' gives the yields of sample B obtained by assuming 100% yield for the photoionization of xenon.

λ(Å)	A	B	C	B'
900	-	-	-	12.6
920	12.6	11.6	11.4	12.2
954	11.2	11.0	-	11.5
973	10.7	10.0	-	10.8
1011	-	9.4	-	9.6
1026	9.6	9.1	8.7	
1048	-	8.1	8.2	
1117	6.6	6.1	5.9	
1161	-	5.2	4.6	
1216	4.1	3.9	3.0	
1277	2.3	2.4	1.6	
1355	0.77	0.85	1.08	
1398	0.37	0.38	0.61	
1436	0.21	0.19	0.46	
1462	0.18	0.15	0.39	
1577	0.07	0.05	0.17	
1608	0.06	0.04	0.14	

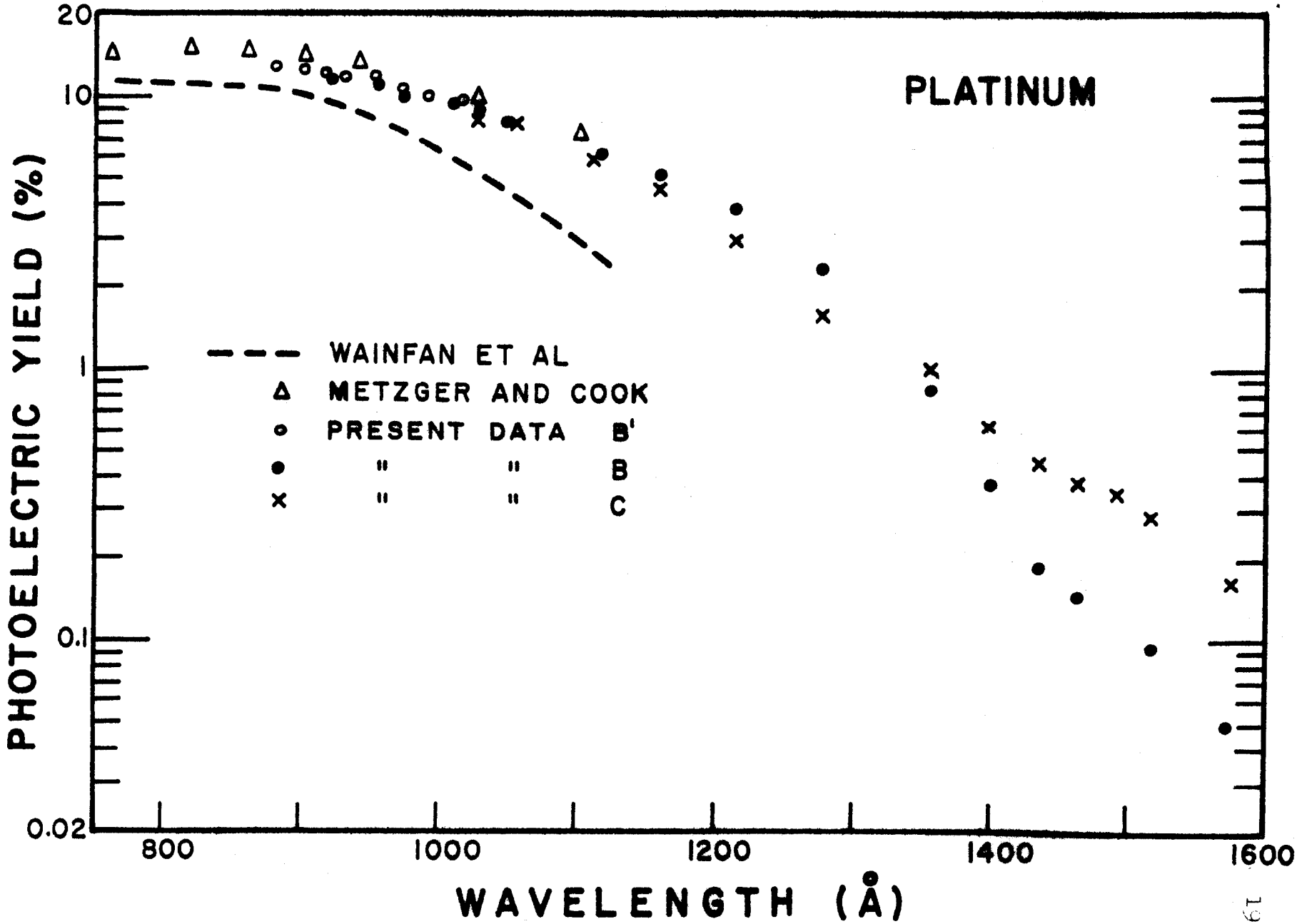

Figure 3. Photoelectric yield of platinum

indium-antimonide, and indium-bismuth. The tabulated values should be regarded as exploratory data, since the vacuum was not very high or clean, and the samples were not properly outgassed. The results show that most untreated metals have yields of 8-15 % at 920 Å, and where comparisons can be made, the results are in agreement with those by Weissler[17] and co-workers. The yields at 1216 Å are in the range 2-4 % but the spread is much larger at 1608 Å. The four semiconductors have somewhat higher yield at wavelengths below 1300 Å; but otherwise, their yield curves are very similar to those of the metals.

2. Photoelectric Yield of Heat Treated Samples

Wainfan, Walker, and Weissler[3,18] have shown that the photoelectric yield of heated metals (Pt, Ta, Ni, Cu, Au, W, Mo, Ag, Pd) are lower than that of untreated samples by a factor of 2 to 4 in the photon energy range 10-25 eV. Furthermore, they observed even lower yields for samples held at elevated temperatures.

The present study supports their work on W, Ta, and Pt for the overlapping region 10-12 eV. Fig. 4 summarizes the photoelectric yield of untreated and heat treated (5 min at 1400°C) tungsten sheets for the region 900-1600 Å (13-6 eV). The result confirms the values obtained by Wainfan et al.[3] in the region 900-1000 Å and extends their work to longer wavelengths. The two curves in Fig. 4 cross at about 1400 Å and the yield of the heat treated sample at 1600 Å is about twice

that of the same sample before heat treatment.

Figs. 5 and 6 show similar results for tantalum and platinum. Our results for tantalum are somewhat lower than those of Wainfan et al.[3] in the overlapping region 900-1000 Å, but the relative heights of the two curves are in good agreement. In the case of platinum our results are somewhat higher than those of Walker et al.[18] in the overlapping region 900-1300 Å. These differences may be ascribed, at least partly, to the differences in the samples. As in the case of tungsten, the solid and broken curves cross at about 1400 Å.

To study the change in photoelectric yield after heat treatment, measurements were made with heat treated samples which were kept in vacuum or exposed to air, O_2, N_2, or He at 1 atm pressure after heat treatment for a period of one to two days. In each case, the "recovery" of photoelectric yield to the value of untreated sample was very slow (no appreciable change to about 30 % of the difference of the two yield curves during a period of one day). The yield curve of a sample which was dipped in water after heat treatment showed the largest recovery.

In agreement with previous experiments, the present study shows that the observed yield of untreated sample is not the characteristic yield of a pure metallic surface. In fact, Knapp and Dutton[7] found the yield of oil contaminated nickel in the region 6-12 eV to be 2 to 6 times that of a sample sealed at 10^{-8} mm Hg. Similarly, Walker et al.[18] observed the yield of untreated nickel to be about an order of

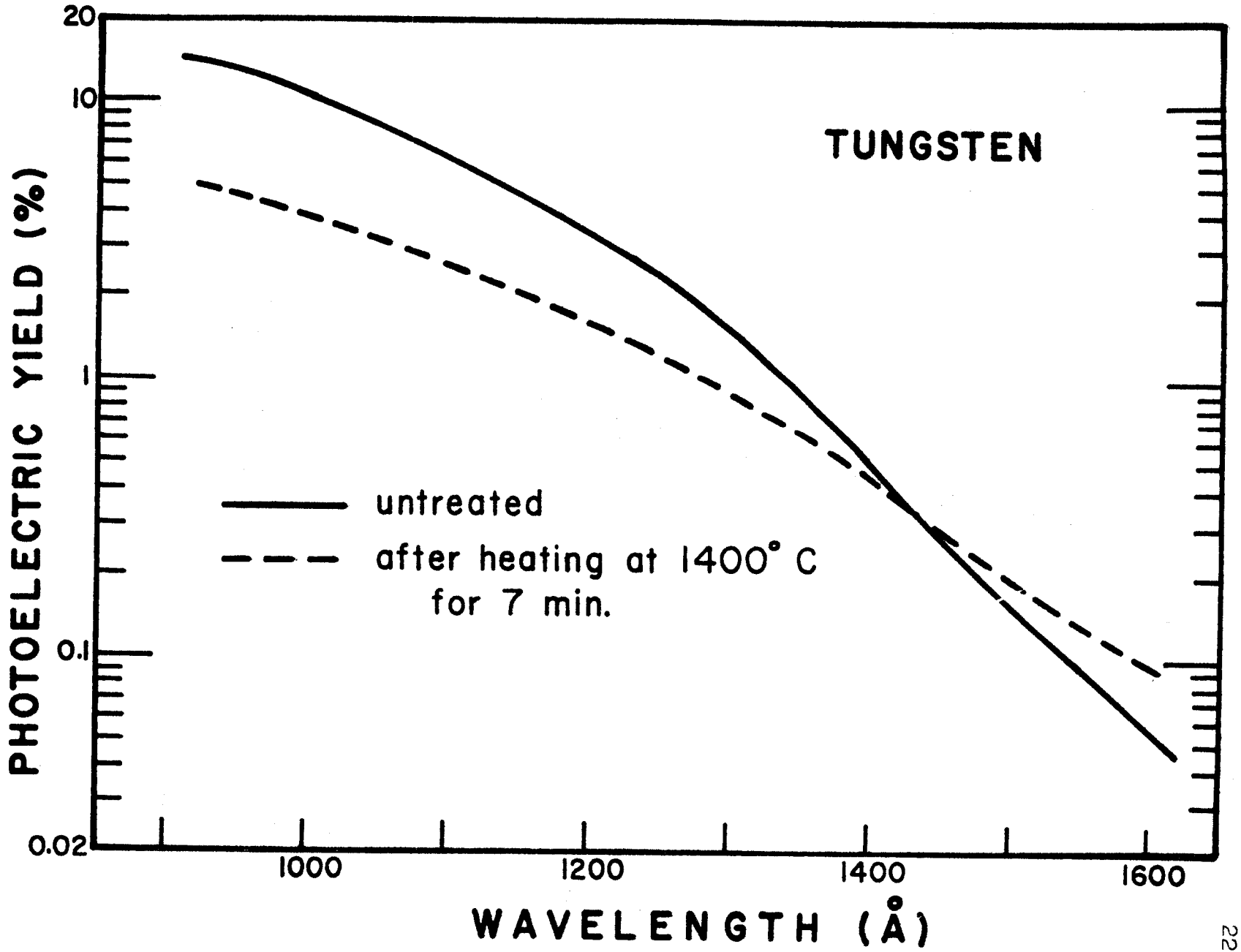

Figure 4. Photoelectric yield of heat-treated tungsten

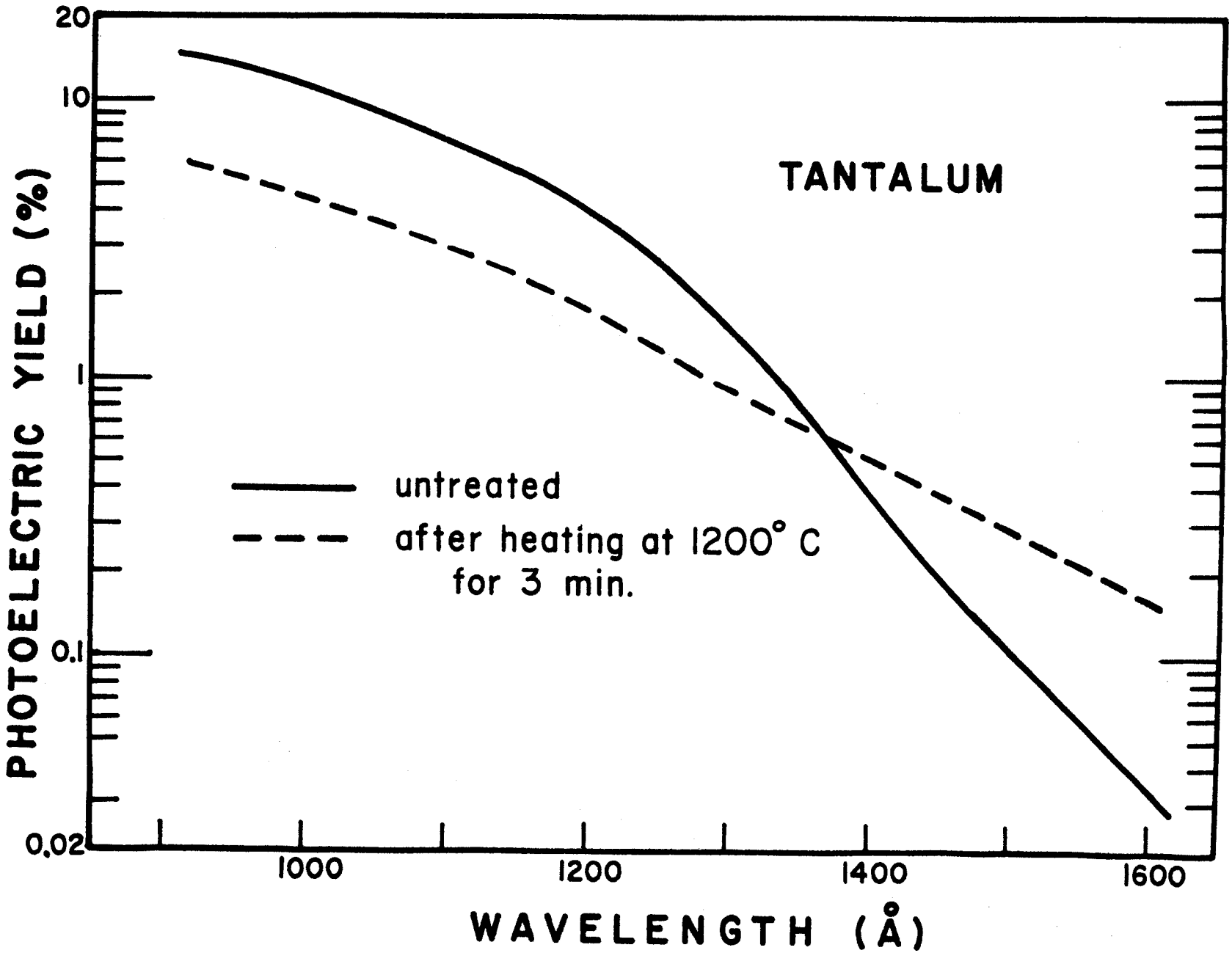

Figure 5. Photoelectric yield of heat-treated tantalum

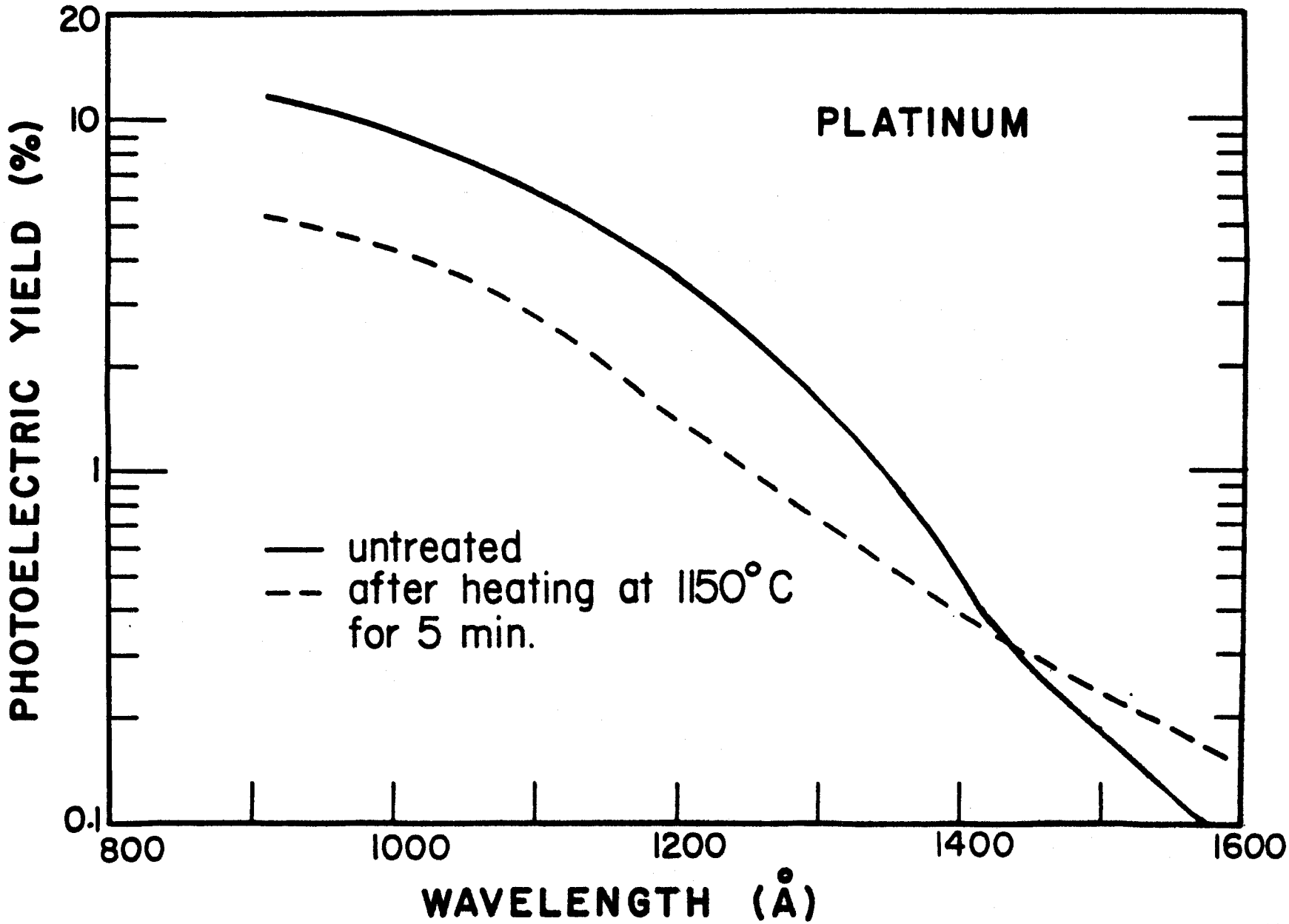

Figure 6. Photoelectric yield of heat-treated platinum

magnitude greater than the yield of a sample held at 900°C.

3. Photoelectric Yield of Gold Black

The photoelectric yield of the gold black deposit on a thermocouple detector element was measured in the manner described in Part II, Section 4. The result is shown in Fig. 7 together with the photoelectric yield of untreated gold sheet. Our results are somewhat higher than the values obtained by Samson[6] in the overlapping region 900-1200 Å. The difference may be ascribed to the difference in samples and also to possible surface contamination. Samson used a collector voltage of 50 V, while we obtained saturation current with 7 V between the gold black and collector. With no collection voltage, Samson observed emission current of about 80 % of the saturation current. A different arrangement was used in the present study so that with no applied voltage, the emission current was about one-tenth of the saturation current. In fact, under this condition the electron emission current was superposed on a somewhat larger reverse (negative) current. The latter was ascribed to photoelectrons from the neighborhood of the slits collected by the gold black surface. In view of the smallness of the net emission current with zero collection voltage, no correction was made to our thermocouple calibration.

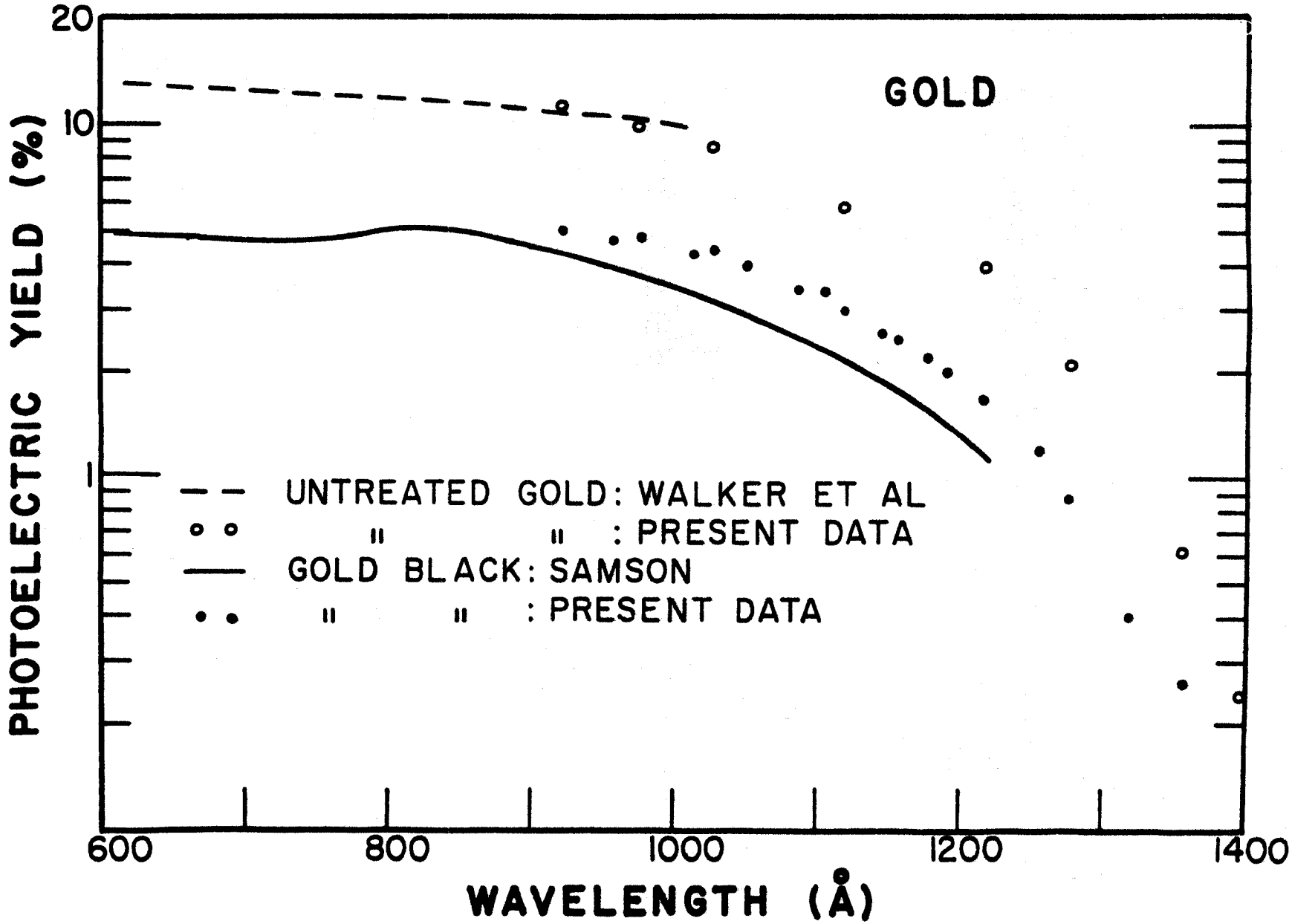

Figure 7. Photoelectric yield of gold and gold black

IV. PHOTOIONIZATION COEFFICIENT OF XENON

Recently several investigators have measured the absorption coefficient of xenon in the spectral region below its ionization threshold (1022 Å). Weissler[23] reported k-values for several wavelengths in the region 400-900 Å. Huffman, Tanaka, and Larrabee[24] and Metzger and Cook[25] using the helium continuum obtained data throughout the region 600-1023 Å. Samson[26] measured k-values at many wavelengths down to 280 Å.

k_i can be equated to k if the assumption that the photoionization yield of rare gases is unity holds throughout the ionization continuum. Wainfan, Walker, and Weissler,[27] however, have reported yields of about 80 % for argon in the region 600-770 Å and lower values in the region 470-600 Å. On the other hand, Samson's determination[6] of a constant relative photoionization yield of rare gases in the region 400-900 Å supports the above assumption.

In the present study we have measured (a) the absolute photoionization yield of xenon in the region 850-1023 Å by means of a thermocouple as described in Part II, Section 3 and (b) the photoionization coefficient with a resolution of 0.2 Å by a method described previously.[9] A more detailed account of the present study was described by Jackson.[28]

1. Absorption Coefficient

The absorption coefficient of xenon in the regions 940-1025 and 850-940 Å are shown in Figs. 8 and 9, respectively. These semilog plots were made by drawing smooth curves through

points at about 230 wavelengths. Each point represents a mean k-value determined with four or more pressures. The experimental uncertainty of the mean k-value at most wavelengths was estimated to be about 5 %, but the uncertainty was larger at some wavelengths where the source intensity was poor or the spectrum poorly resolved. The mean k-values are also tabulated in Appendix II.

As shown in Fig. 8, the absorption in the region 940-1022 Å consists of several very broad lines overlapping a possible ionization continuum with threshold at 1022 Å ($^2P_{3/2}$ level). According to Beutler[29] these broadened lines are members of Rydberg series $(5p)^5$ md←$(5p)^6$ converging to the upper doublet state $^2P_{1/2}$ of the ion at 923 Å. Absorption coefficients for these "Beutler lines" range from 4100 cm^{-1} at 995.8 Å (m = 6) to 3420 cm^{-1} at 930.8 Å (m = 13).

A member (m = 8) of the second Rydberg series $(5p)^5$ ms←$(5p)^6$ observed by Beutler is superimposed on the first diffuse line at 985 Å. The second member was detected by Huffman *et al.*[24] and by Metzger and Cook,[25] but we were unable to resolve it clearly with the hydrogen source.

The minimum k-value between the diffuse lines increases with decreasing wavelength. This increase is probably due to increasing overlapping of the wings of the lines. Hence, the level of the ionization continuum may be significantly lower than the minimum k-value of 290 cm^{-1} at 1002 Å.

The peak near the $^2P_{3/2}$ threshold is much higher than the level of the first continuum ($k \sim 290$ cm^{-1}) and it appears

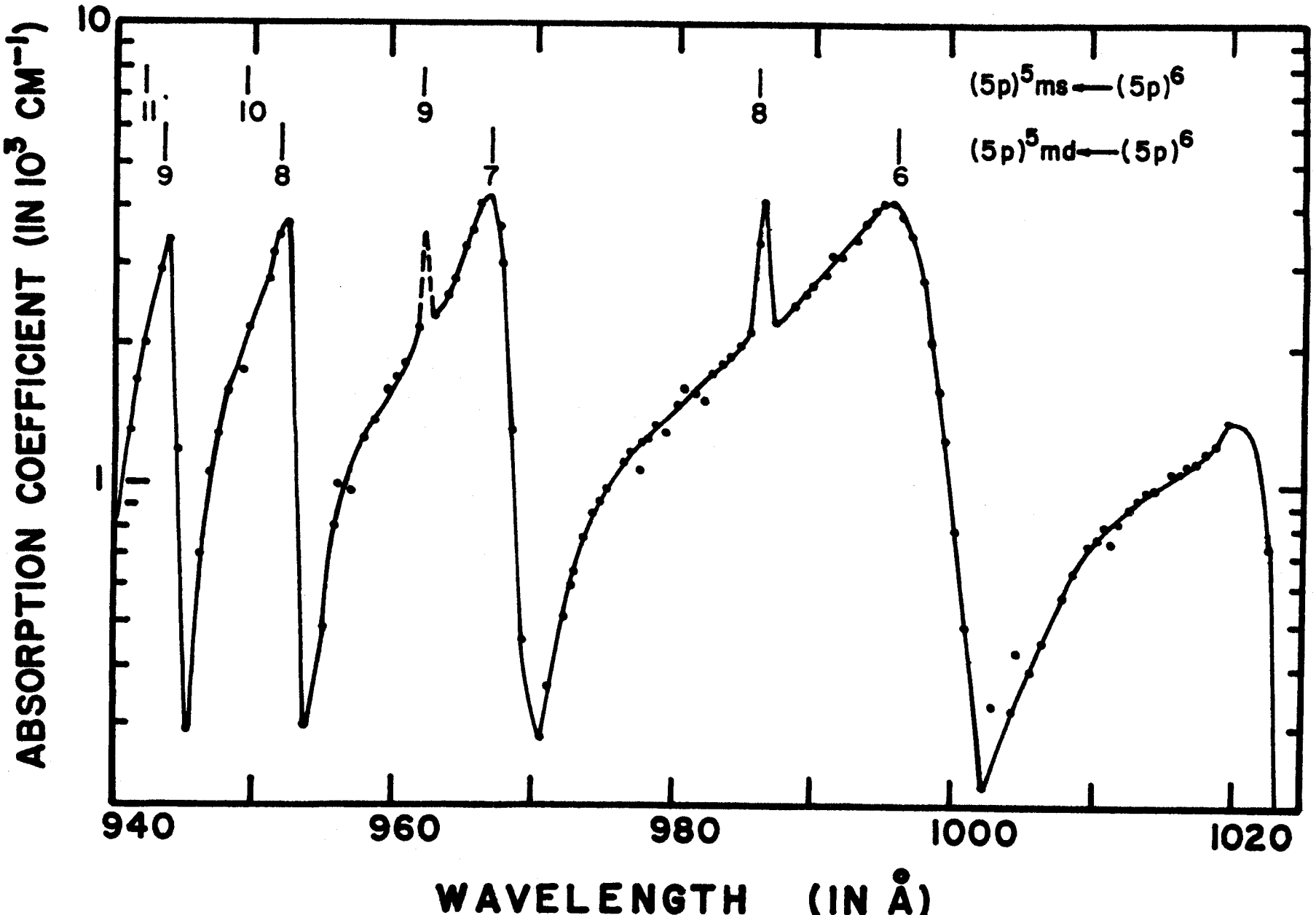

Figure 8. Absorption coefficient of xenon from 940 to 1022 Å

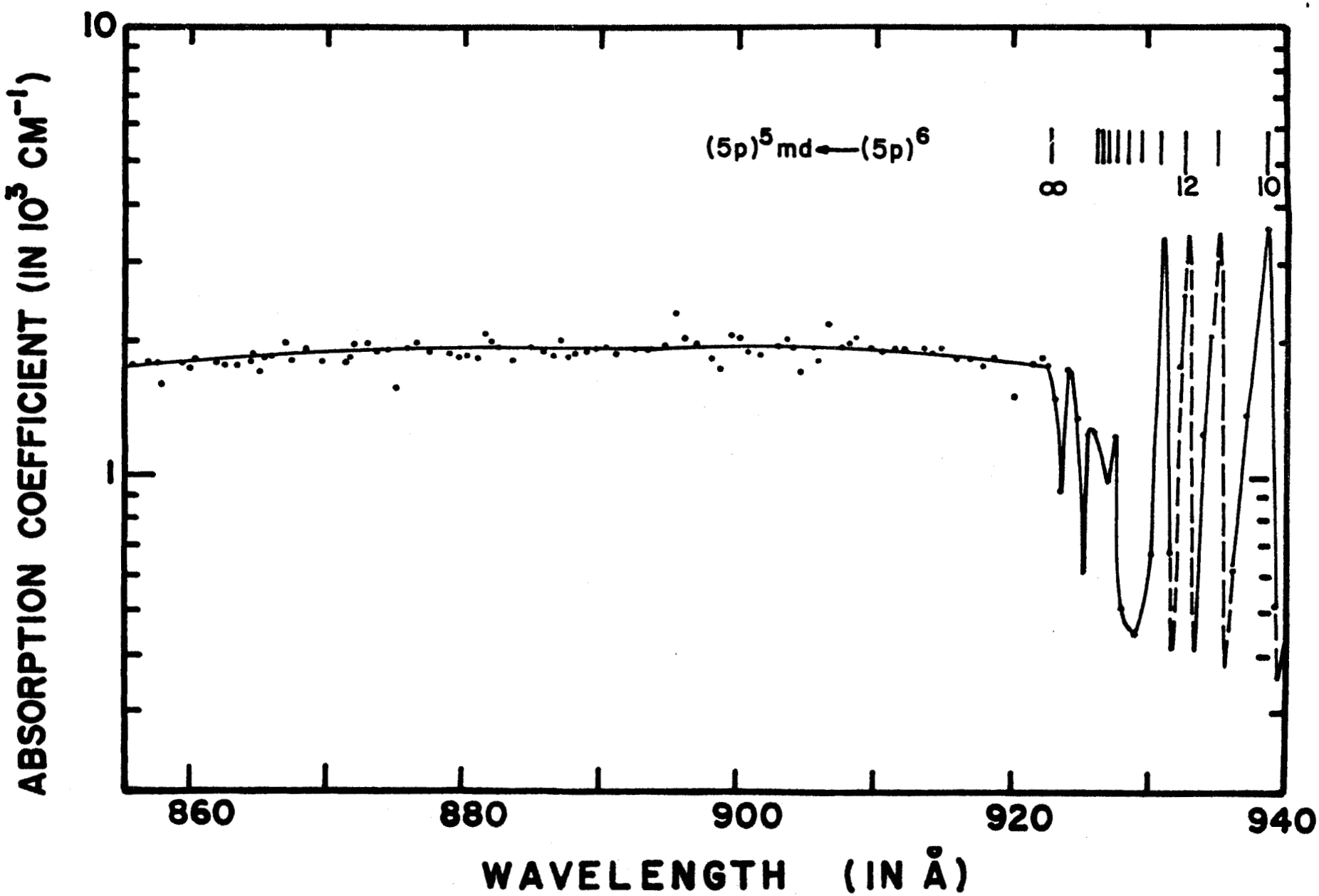

Figure 9. Absorption coefficient of xenon from 855 to 940 Å

as another diffuse line. The strong absorption in the region 1002-1022 Å is probably due to preionization involving the transition $(5p)^5\ 5d \leftarrow (5p)^6$, although this line is at about 1069 Å, some 47 Å beyond the ionization threshold. This preionization is apparently a form of configuration interaction.[30]

Fig. 9 shows that the absorption spectrum below 923 Å is a rather flat continuum as reported by others.[24-26] Our result for the region near the convergence limit of the two Rydberg series is incomplete because a continuous source was not used.

Some of the k-values obtained by other investigators are tabulated in Table II. The present results in the region 1020-850 Å are consistently lower than the values obtained by Huffman et al.[24] by 10 to 20 per cent. On the other hand, the present results are a little higher than those obtained by Metzger and Cook.[25] These differences may be attributed largely to systematic errors in pressure measurement of flowing gas.

2. Photoionization Yield

The photoionization yield of xenon is shown in Fig. 10. Each point represents the mean of three or more yields obtained with different gas pressures. These values are also tabulated in Appendix II. About 85 % of the mean yields lie in the range 100±5 %. The larger spread of values in the region 923-928 Å may be ascribed to the incomplete resolution of the higher members of the Rydberg series. The large

Table II Comparison of Absorption Coefficient (cm^{-1}) of Xenon at Some Wavelengths

λ(Å)	Huffman[a]	Metzger[b]	Samson[c]	Weissler[d]	Present
1020	1500	650			1410
1002	350	350			290
995	5100	3500			4100
970	350	200			290
966	4900	3500			4100
954	400	330			300
920	2100	1800	1680	1650	1800
850	1930	1600	1560	1550	1700
700	1500	1200	1200	1250	
600	1050	700	830	900	
500			400	550	

a. R. E. Huffman, Y. Tanaka, and J. C. Larrabee, J. Chem. Phys. 39, 902 (1963).

b. P. H. Metzger and G. R. Cook (private communication).

c. J. A. R. Samson (to be published).

d. G. L. Weissler, J. Quant. Spectry. Radiative Transfer 2, 383 (1962).

scatter of value below 880 Å was due to the low intensity of the light source.

The present result shows that the photoionization yield of xenon is unity in the region 860-1020 Å which includes the preionized Beutler lines. By combining this result with the data obtained by Samson,[6] we may conclude that the photoionization yield of xenon, krypton, argon and neon is unity at least down to 450 Å.

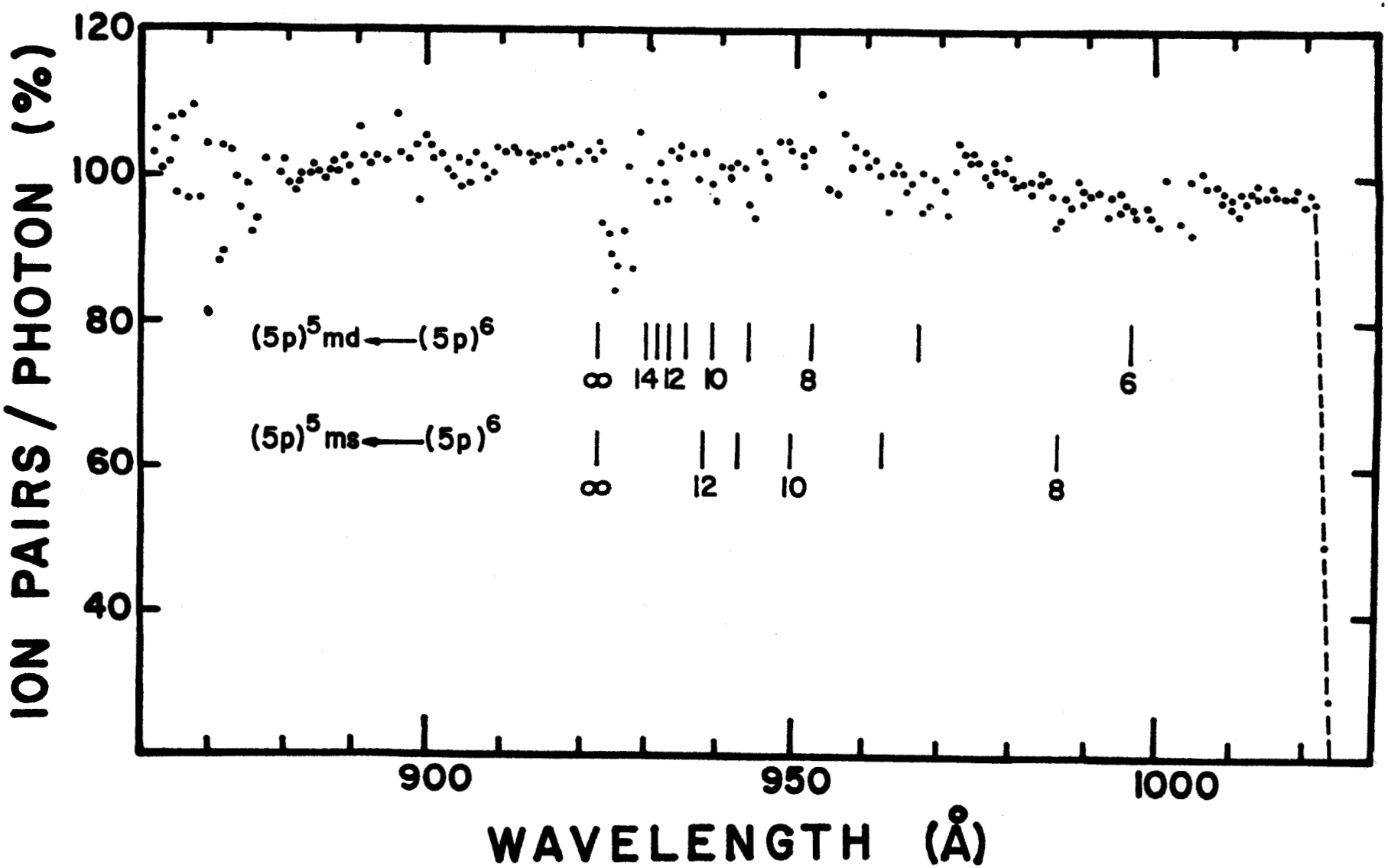

Figure 10. Photoionization yield of xenon from 860 to 1022 Å

V. PHOTOIONIZATION YIELD OF NITRIC OXIDE

In Part V we are primarily concerned with the photoionization yield of nitric oxide. The total absorption cross section of NO in the vuv region has been studied by a number of investigators, and their papers have been reviewed by Weissler[17] and Watanabe.[31] Photoionization yield of NO in the region 1050-1350 Å was first reported by Watanabe, Marmo and Inn[32] and revised by Watanabe.[8] Some yield values in the region below 1000 Å were published by Walker and Weissler.[33]

The photoionization yield of NO at about 470 wavelength in the region 850-1345 Å was determined by the method described in Part II, Section 3. With the cell length (27.1 cm) and gas pressures (up to 0.4 mm Hg) used the absorption was usually incomplete so that the observed ion current was multiplied by the factor $I_o/(I_o-I)$, where I was computed from the previously determined absorption coefficient[34] of NO.

The yield of NO is summarized in Table III. Each value represents a mean value of data obtained with three or more pressures. In the region 850-1010 Å, most of the yield value lie in the range 30-60 %. Higher yields, 50-90 %, were observed in the region 1010-1260 Å. The results for the region 1050-1345 Å agree within experimental errors with previous results[8] but are consistently lower by several percent. At shorter wavelengths the results are in fair agreement with the work of Walker and Weissler[33] although a close comparison is not possible.

Table III Photoionization Yield Y(in %) of Nitric Oxide in the Region 850-1345 Å

λ(Å)	Y	λ(Å)	Y	λ(Å)	Y
849.1	51.3	876.0	48.7	900.6	39.6
850.4	40.6	877.4	48.4	901.7	43.0
851.5	39.8	879.0	44.5	902.7	42.3
852.2	38.3	880.1	48.2	904.1	43.2
852.8	34.3	881.0	46.6	905.5	39.3
854.1	47.8	881.9	47.9	906.8	29.7
855.7	39.9	882.5	47.6	907.6	32.5
856.1	44.6	883.5	50.1	908.5	38.5
857.0	57.0	885.0	54.4	909.5	42.9
857.6	57.2	885.8	56.2	910.6	39.5
859.8	44.8	886.5	57.1	911.4	38.2
862.1	31.8	888.1	45.1	912.1	37.4
862.6	33.7	889.0	23.7	913.4	34.0
863.4	48.0	889.8	24.3	914.2	34.6
864.9	61.5	891.2	46.0	914.8	34.9
865.8	52.3	892.5	52.2	916.0	32.8
867.4	54.5	893.5	52.7	917.0	29.1
869.5	38.6	894.5	52.4	917.8	25.1
871.4	48.8	895.5	52.1	919.0	24.8
872.1	45.8	896.1	59.9	920.0	28.7
872.9	50.8	897.1	41.9	921.4	39.0
873.6	53.1	898.1	44.1	922.3	46.2
875.1	52.7	899.6	35.6	923.4	50.0

λ(Å)	Y	λ(Å)	Y	λ(Å)	Y
924.0	50.2	946.7	56.1	974.6	49.1
925.1	49.0	948.1	54.1	976.2	53.9
926.0	50.9	949.1	51.0	976.7	56.9
926.8	51.0	949.7	47.6	977.5	60.2
927.8	48.9	950.9	45.9	978.5	58.4
928.8	42.6	952.3	49.5	979.2	54.1
930.0	34.7	953.7	61.0	980.1	55.2
931.0	28.5	954.8	59.9	981.3	71.4
931.4	29.3	955.7	54.6	982.1	75.8
932.5	32.8	956.9	51.2	983.8	66.2
933.3	38.5	957.8	53.2	984.6	58.6
933.8	41.3	958.4	51.1	986.1	51.9
934.5	44.0	960.0	52.4	986.9	51.9
936.1	48.8	960.7	54.8	988.5	51.5
936.9	50.4	961.7	50.2	989.6	51.5
937.6	51.0	962.8	44.9	990.6	49.4
938.8	53.2	964.1	48.6	991.7	48.7
940.3	60.8	964.8	51.9	993.3	53.2
941.1	58.9	966.0	57.6	994.2	53.3
941.6	53.5	967.5	60.3	995.2	55.4
942.2	53.8	968.3	58.6	996.1	52.3
943.3	52.9	969.2	56.7	996.6	58.0
944.8	56.4	970.3	52.9	997.6	63.3
945.2	57.2	972.5	47.6	998.8	58.1
946.0	57.4	973.4	47.6	1000.0	57.0

λ(Å)	Y	λ(Å)	Y	λ(Å)	Y
1000.7	59.2	1027.1	55.7	1050.6	62.9
1001.9	60.9	1028.2	60.6	1052.4	59.9
1002.6	57.0	1029.3	68.5	1054.2	66.1
1004.0	53.3	1030.2	71.8	1054.7	69.5
1004.6	52.0	1030.8	71.7	1055.5	70.1
1005.5	51.0	1031.9	61.5	1056.4	67.8
1006.2	49.5	1033.6	67.3	1058.8	63.7
1007.6	48.5	1034.3	68.5	1059.5	67.4
1008.8	47.6	1035.5	62.8	1061.7	63.9
1009.4	47.5	1036.5	57.8	1062.6	58.5
1010.0	46.9	1037.2	59.3	1063.6	57.0
1010.8	49.5	1038.1	60.2	1065.1	64.9
1011.5	53.4	1039.1	63.5	1066.4	70.8
1012.3	63.9	1039.9	66.9	1067.0	70.7
1013.5	62.0	1040.9	61.3	1067.6	72.2
1014.2	59.0	1042.5	65.2	1068.5	72.5
1016.0	55.7	1042.9	62.3	1068.9	70.4
1016.9	53.7	1043.5	60.9	1069.9	68.0
1017.8	52.3	1044.1	58.4	1070.7	64.4
1019.4	60.3	1045.3	61.7	1071.4	63.8
1020.8	66.1	1046.6	66.4	1072.2	62.4
1022.4	54.5	1047.1	67.9	1072.7	61.8
1023.4	52.9	1047.8	72.6	1073.2	61.1
1024.7	50.9	1049.5	70.1	1073.9	61.1
1025.7	51.8	1050.1	65.6	1075.3	63.5

λ(Å)	Y	λ(Å)	Y	λ(Å)	Y
1076.0	64.4	1107.3	78.7	1133.5	84.5
1077.0	65.7	1108.3	83.0	1134.3	77.9
1077.8	69.6	1108.7	82.4	1135.4	71.8
1079.8	69.1	1109.9	82.5	1136.0	70.0
1081.6	70.9	1110.4	80.5	1136.6	66.6
1083.0	75.0	1111.5	77.2	1137.5	63.2
1084.6	64.3	1112.3	74.1	1138.9	69.1
1086.1	67.8	1113.0	73.3	1139.5	74.6
1086.8	74.2	1113.9	76.5	1141.8	71.1
1087.7	78.7	1114.4	77.2	1143.1	70.7
1088.7	75.8	1115.1	74.3	1144.5	72.0
1090.0	73.4	1116.5	75.1	1145.3	73.6
1091.1	71.5	1117.6	74.6	1146.0	76.4
1091.7	72.0	1119.2	76.7	1147.0	73.4
1092.7	72.0	1121.3	76.7	1147.8	71.3
1093.4	70.6	1122.4	76.8	1148.6	77.9
1094.6	71.0	1123.8	77.0	1150.1	73.7
1095.9	69.5	1125.1	78.4	1150.9	80.2
1097.1	70.5	1125.9	78.6	1151.9	79.6
1097.9	70.6	1127.2	81.9	1153.1	74.1
1099.5	76.7	1127.9	84.0	1153.7	75.3
1100.5	75.8	1129.0	81.2	1154.7	77.0
1102.1	77.4	1130.4	83.0	1156.2	75.0
1104.4	84.5	1131.4	84.5	1157.1	73.5
1105.9	80.1	1132.8	86.6	1158.3	72.8

λ(Å)	Y	λ(Å)	Y	λ(Å)	Y
1158.7	81.2	1184.3	83.8	1208.9	79.7
1159.9	80.3	1185.0	79.5	1210.7	79.9
1160.7	78.6	1185.7	75.1	1211.4	84.0
1161.3	85.3	1186.6	74.2	1212.9	77.6
1162.3	84.8	1187.1	75.9	1214.0	70.0
1163.0	81.8	1187.8	80.8	1215.7	77.7
1163.8	85.4	1189.4	85.2	1217.4	79.8
1164.9	77.2	1190.3	81.5	1219.0	76.9
1166.1	82.4	1191.0	77.7	1219.9	82.9
1167.0	77.8	1191.8	87.0	1221.2	82.2
1168.4	80.6	1193.3	85.5	1222.9	75.6
1168.9	79.5	1194.6	85.9	1223.6	86.0
1169.7	74.8	1195.7	82.9	1224.9	76.1
1170.6	72.4	1198.3	83.6	1225.6	78.0
1172.2	75.8	1198.9	81.0	1226.1	76.9
1173.2	70.2	1199.4	80.5	1227.2	70.5
1174.5	79.5	1199.9	80.0	1228.3	78.9
1175.9	80.8	1200.6	77.4	1230.1	78.6
1176.8	84.5	1201.8	82.5	1230.9	74.8
1178.3	83.7	1202.6	84.6	1232.1	71.9
1180.5	85.5	1203.9	81.8	1233.2	66.7
1181.4	84.6	1205.0	86.2	1234.2	71.8
1182.0	84.5	1206.1	83.7	1235.7	72.0
1182.5	86.4	1206.7	85.0	1236.4	66.2
1183.1	85.6	1207.5	87.6	1236.9	67.5

λ(Å)	Y	λ(Å)	Y	λ(Å)	Y
1238.0	71.7	1261.8	57.2	1287.9	32.7
1239.7	77.5	1262.9	51.3	1289.4	38.4
1240.4	76.5	1263.6	51.6	1290.3	46.6
1241.4	74.1	1264.3	53.3	1291.1	49.5
1243.5	74.2	1265.7	47.0	1292.0	44.7
1244.5	62.5	1266.5	43.8	1292.6	42.8
1245.9	72.5	1267.2	45.7	1293.4	41.4
1247.4	73.6	1268.1	37.7	1294.6	35.5
1248.0	68.1	1268.9	40.5	1295.5	43.1
1248.9	61.1	1269.7	48.3	1297.3	42.2
1249.8	55.0	1270.6	43.3	1298.2	39.5
1250.4	56.6	1271.4	46.3	1299.0	33.1
1251.0	58.6	1272.0	46.4	1299.9	33.0
1252.1	65.9	1273.2	44.1	1301.8	26.5
1253.1	67.8	1274.1	42.0	1302.4	26.3
1253.7	73.0	1274.6	47.0	1304.1	21.4
1254.8	69.5	1275.8	52.9	1305.0	20.2
1255.5	70.3	1276.7	47.0	1305.5	17.7
1256.5	68.3	1278.1	53.8	1306.5	17.5
1256.8	64.5	1279.6	51.3	1307.5	19.9
1257.2	65.9	1281.1	45.0	1308.7	20.8
1257.9	67.6	1283.1	39.4	1309.8	19.6
1258.8	62.5	1284.3	31.5	1311.0	20.7
1259.2	63.8	1285.8	27.8	1312.3	20.0
1259.9	64.9	1286.5	30.3	1312.9	21.1

λ(Å)	Y	λ(Å)	Y	λ(Å)	Y
1314.7	23.8	1323.3	13.9	1334.1	17.6
1215.4	24.1	1325.0	13.6	1335.0	16.5
1316.6	25.6	1325.8	11.2	1335.8	15.4
1317.1	23.6	1327.0	15.0	1337.3	19.6
1317.9	22.4	1327.5	14.0	1338.4	17.9
1319.0	21.1	1329.1	20.9	1339.7	12.9
1320.2	16.6	1330.2	19.8	1340.7	5.7
1320.7	17.6	1331.0	19.7	1342.0	2.4
1321.3	17.7	1332.5	12.0	1343.3	2.0
1322.3	12.1	1333.7	16.6	1345.0	0.6

The result for Lyman alpha (1215.7 Å) is of interest to investigators who use nitric oxide ion chambers. The present value for this line is 78±5 % which is somewhat lower than the value of 83 % reported previously.[8] However, within experimental error the results are in agreement and there appears to be no reason to revise the recommended value[34] of 81 %. Some of the discrepancies may be explained by the fact the resolution used in the present work is about three times better than our previous work[8] and the yield curve shows considerable amount of structure.

VI. CONCLUSIONS

The present work supports the suggestion by Samson[6] that a rare-gas ion chamber is the most convenient device to determine absolute intensities in the vuv region below 1000 Å. He found a constant relative photoionization yield of xenon, krypton, argon, and neon in the region 400-900 Å. The present result shows that the absolute yield of xenon is unity in the region 850-1020 Å. This type of ion chamber does not have a long wavelength scattered light response which is encountered in thermocouple measurements.

Thermocouples are still useful for the vuv region from 1000-2000 Å where a suitable gas ion chamber is not available for the entire spectral range. A thermocouple can be calibrated in the 800-1000 Å region with a xenon gas ion chamber and then used in the region 1000-2000 Å. This procedure is simpler and more reliable than the previous one which requires (a) calibration in the visible region, (b) measurement of vacuum-to-air response ratio, and (c) the assumption that its blackness is the same in the visible and the vuv regions.

Curves of photoelectric yield of 23 metals and 4 semiconductors in the region 900-2000 Å show no structure. These curves are very similar to results reported previously. The result for heat-treated samples also confirms the work of Weissler and co-workers. A preliminary study showed that yield curves are changed appreciably by using clean high vacuum, but a more systematic study is desirable.

A remeasurement of the photoionization yield of NO with improved resolution generally confirmed previous results. In particular, the recommended yield value at the wavelength of Lyman alpha is 81 %.

ACKNOWLEDGMENTS

We are greatly indebted to Dr. S. P. Sood and Mr. Robert Nakata for assistance in obtaining absorption data, to Mr. James S. Sasser* for assistance in computation and analysis of the NO data, to Mr. Daniel Katayama* and Mr. Kevin S. Fansler* for photoelectric measurements and to Mr. George Yokotake for fabrication of various parts.

---

* Participants in a course on Directed Research.

REFERENCES

1. D. M. Packer and C. Lock, J. Opt. Soc. Am., 41, 699 (1951).
2. K. Watanabe and E. C. Y. Inn, J. Opt. Soc. Am., 43, 32 (1953).
3. N. Wainfan, W. C. Walker, and G. L. Weissler, J. Appl. Phys. 24, 1318 (1953).
4. F. S. Johnson, K. Watanabe, and R. Tousey, J. Opt. Soc. Am., 41, 702, (1951).
5. A. M. Smith, Thesis, University of Rochester, 1961; A. Smith and D. Dutton, J. Phys. Chem. Solids, 22, 315 (1961).
6. J. A. R. Samson, J. Opt. Soc. Am., 54, 6 (1964).
7. R. A. Knapp and D. B. Dutton, Technical Note No. 1, Institute of Optics, University of Rochester, (1963).
8. K. Watanabe, J. Chem. Phys., 22, 1564 (1954).
9. K. Watanabe and F. F. Marmo, J. Chem. Phys., 25, 965 (1956).
10. A. P. Lukirskii, M. A. Rumsh, and L. A. Smirnov, Optics and Spectry., 9, 262 (1960).
11. E. Hinnov and F. W. Hoffmann, J. Opt. Soc. Am., 53, 1259 (1963).
12. G. Haas and R. Tousey, J. Opt. Soc. Am., 49, 593 (1959).
13. K. Watanabe and J. R. Mottl, in Threshold of Space, edited by M. Zelikoff (Pergamon Press, London, 1957) p. 151.
14. K. Watanabe, J. Opt. Soc. Am., 43, 318 (1953).
15. J. Lee and H. H. Seliger, J. Chem. Phys., 40, 519 (1964).
16. L. Harris, R. T. McGinnes, and B. M. Siegel, J. Opt. Soc. Am., 38, 582 (1948).
17. G. L. Weissler, Handbuch der Physik (Springer Verlag, Berlin, 1956) Vol. XXI, Chap. 24.
18. W. C. Walker, N. Wainfan, and G. L. Weissler, J. Appl. Phys., 26, 1366 (1955).
19. W. C. Walker, O. P. Rustgi, and G. L. Weissler, J. Opt. Soc. Am., 49, 471 (1959).
20. H. E. Hinteregger, Phys. Rev., 96, 538 (1954).

21. H. E. Hinteregger and K. Watanabe, J. Opt. Soc. Am., 43, 604 (1953).

22. P. H. Metzger and G. R. Cook (private communication).

23. G. L. Weissler, J. Quant. Spectry. Radiative Transfer, 2, 383 (1962).

24. R. E. Huffman, Y. Tanaka, and J. R. Larrabee, J. Chem. Phys., 39, 902 (1963).

25. P. H. Metzger and G. R. Cook (to be published).

26. J. A. R. Samson (to be published).

27. N. Wainfan, W. C. Walker, and G. L. Weissler, Phys. Rev., 99, 542 (1955).

28. R. S. Jackson, Thesis, University of Hawaii, 1963.

29. H. Beutler, Zeit. fur Physik, 86, 710 (1933).

30. U. Fano, Phys. Rev., 124, 1866 (1961).

31. K. Watanabe, in Advances of Geophysics (Academic Press, New York, 1958) Vol. 5, p. 155.

32. K. Watanabe, F. F. Marmo, and E. C. Y. Inn, Phys. Rev., 91, 1155 (1953).

33. W. C. Walker and G. L. Weissler, J. Chem. Phys., 23, 1962 (1955).

34. K. Watanabe (unpublished material).

APPENDIX I

Photoelectric Yield (in %) of
Some Metals and Semiconductors

λ(Å)	Aluminum	Beryllium	Cadmium	Cobalt
920	15.3	14.5	9.3	10.6
973	-	11.2	-	-
1026	10.3	9.4	7.4	7.5
1048	10.0	8.9	6.6	6.4
1105	7.9	8.0	4.9	5.0
1117	7.4	7.8	4.2	4.8
1147	6.6	5.6	3.6	4.2
1161	5.9	5.0	3.2	3.9
1176	5.5	4.5	2.9	3.5
1190	4.8	4.2	2.6	3.2
1216	4.0	3.3	2.2	2.6
1254	3.0	2.2	1.50	1.88
1277	2.3	1.90	1.18	1.51
1355	1.54	0.74	0.56	0.64
1398	0.94	0.58	0.35	0.42
1436	0.76	0.33	0.23	0.30
1462	0.67	0.26	0.18	0.24
1491	0.35	0.20	0.14	0.19
1519	0.29	0.14	0.10	0.15
1577	0.15	0.066	0.056	0.090
1608	0.12	0.046	0.036	0.069
1700		0.030	0.012	0.015
1800		0.018	0.006	
1900		0.015		

λ(Å)	Copper	Gold	Indium	Iron
920	8.9	11.4	11.2	10.2
973	-	9.7	-	
1026	7.6	8.6	8.4	8.0
1048	7.0	-	8.5	7.4
1105	5.6	-	7.8	5.8
1117	5.2	5.9	7.6	5.5
1147	4.7	-	7.2	4.9
1161	4.2	-	6.6	4.6
1176	3.9	-	6.2	4.1
1190	3.6	-	5.5	3.8
1216	3.3	3.9	5.9	3.3
1254	2.2	-	4.0	2.4
1277	1.84	2.1	3.2	1.80
1355	0.85	0.65	1.37	0.99
1398	0.49	-	0.75	0.47
1436	0.33	0.27	0.44	0.37
1462	0.29	-	0.31	0.29
1491	0.25	-	0.22	0.25
1519	0.21	0.112	0.17	0.20
1577	0.16		0.11	0.17
1608	0.14	0.106	0.091	0.09
1700	0.076	0.077	0.051	
1800	0.048	0.053	0.034	
1900	0.025	0.045	0.022	
2000	0.013	0.027	0.010	

λ(Å)	Lead	Magnesium	Molybdenum	Nickel
920	8.3	9.8	12.0	10.9
973	-	-	-	9.1
1026	6.3	8.1	8.8	8.8
1048	5.5	7.2	8.4	7.6
1105	4.3	5.7	6.5	5.6
1117	4.2	5.4	6.3	5.3
1147	3.6	5.0	5.6	4.6
1161	3.4	4.6	5.4	4.3
1176	3.0	4.4	4.9	3.9
1190	2.8	3.9	4.5	3.5
1216	3.2	3.5	3.8	3.0
1254	2.4	2.8	2.7	2.3
1277	2.0	2.3	2.0	1.8
1355	1.20	1.16	0.99	0.84
1398	0.89	0.64	0.41	0.50
1436	0.66	0.53	0.31	0.32
1462	0.56	0.43	0.24	0.26
1491	0.43	0.36	0.22	0.20
1519	0.34	0.33	0.18	0.16
1577	0.20	0.17	0.10	0.10
1608	0.15	0.14	0.086	0.072
1700	0.055			0.023
1800				0.018
1900				0.007

λ(Å)	Niobium	Palladium	Platinum	Silver
920	11.9	10.9	11.4	8.9
973	-	9.2	9.9	-
1026	9.5	8.2	8.7	7.1
1048	8.7	-	8.2	6.3
1105	6.2	-	6.2	4.9
1117	5.4	5.3	5.9	4.4
1147	4.5	-	5.0	4.1
1161	4.2	-	4.6	3.9
1176	3.8	-	4.1	3.7
1190	3.4	-	3.7	3.3
1216	3.2	3.5	3.0	2.9
1254	2.3	-	2.2	2.2
1277	1.9	1.9	1.9	1.9
1355	0.80	0.69	1.08	1.05
1348	0.35	-	0.61	0.80
1436	0.27	0.37	0.46	0.64
1462	0.20	-	0.39	0.53
1491	0.14	-	0.35	0.42
1519	0.10	0.21	0.29	0.34
1577	0.054	-	0.17	0.22
1608	0.037	0.15	0.14	0.18
1700	0.013	0.08	0.065	0.17
1800		0.02	0.047	0.14
1900			0.033	0.08
2000			0.025	0.05

λ(Å)	Tantalum	Thorium	Tin	Titanium
920	14.5	10.4	13.6	13.5
973	-	-	-	-
1021	10.0	8.0	9.5	11.0
1048	8.3	7.3	8.0	9.2
1105	7.0	4.9	6.5	7.2
1117	6.5	4.3	6.1	7.0
1147	5.6	3.6	5.2	5.8
1161	5.1	3.3	4.7	5.3
1176	4.5	3.0	4.2	4.7
1190	4.2	2.6	3.8	4.2
1216	3.6	2.2	3.5	3.6
1254	2.4	1.6	2.5	2.5
1277	1.9	1.30	1.9	1.9
1355	0.80	0.53	0.93	0.71
1398	0.39	0.31	0.54	0.36
1436	0.22	0.20	0.35	0.21
1462	0.16	0.14	0.28	0.15
1491	0.12	0.087	0.21	0.11
1519	0.088	0.056	0.17	0.081
1577	0.047	0.036	0.10	0.045
1608	0.029	0.028	0.072	0.031
1700		0.005	0.045	0.008
1800			0.032	
1900			0.012	

λ(Å)	Tungsten	Vanadium	Zinc	Zirconium
920	13.9	10.1	9.4	11.9
973	10.7	-	-	-
1026	9.0	7.0	5.5	9.4
1048	8.1	6.3	4.7	8.5
1105	6.1	4.6	3.7	5.8
1117	5.8	4.2	3.2	5.1
1147	4.6	3.8	2.6	4.2
1161	4.1	3.6	2.3	3.8
1176	3.9	3.5	2.1	3.5
1190	3.5	3.1	1.8	3.1
1216	3.0	3.2	1.7	2.6
1254	2.2	2.4	1.28	1.9
1277	1.93	2.0	1.07	1.56
1355	0.85	0.74	0.43	0.57
1398	0.49	0.34	0.26	0.28
1436	0.33	0.17	0.17	0.17
1462	0.26	0.11	0.13	0.11
1491	0.19	0.078	0.076	0.058
1577	0.07	0.032	0.050	0.037
1608	0.05	0.024	0.041	0.032
1700		0.009	0.012	
1800		0.007		

λ(Å)	Gallium Antimonide	Germanium	Indium Antimonide	Indium Bismuth
920	19.0	19.9	15.3	17.7
973	-	-	-	-
1026	11.2	13.1	10.4	11.0
1048	10.3	12.2	9.9	9.9
1105	8.4	8.9	7.5	8.4
1117	7.8	8.1	7.0	7.6
1147	7.1	7.7	7.0	6.8
1161	6.9	7.2	6.6	6.6
1176	6.1	6.6	6.3	5.9
1190	5.7	6.1	5.9	5.2
1216	4.7	5.0	5.1	4.9
1254	3.5	3.5	3.8	3.4
1277	2.8	2.8	3.0	2.9
1355	1.13	1.18	1.08	1.37
1398	0.60	0.69	0.42	0.86
1426	0.36	0.51	0.24	0.57
1462	0.27	0.44	0.20	0.43
1491	0.19	0.38	0.17	0.32
1519	0.15	0.33	0.15	0.25
1577	0.087	0.23	0.08	0.15
1608	0.066	0.18	0.06	0.11
1700	0.021			0.055
1800	0.011			0.037
1900	0.005			0.018

APPENDIX II

Absorption Coefficient and Photoionization Yield of Xenon

λ in A	k in $10^3 cm^{-1}$	Yield in %	λ in A	k in $10^3 cm^{-1}$	Yield in %
1024.7	.066		1009.4	.745	97.7
1024.3	.333		1008.7	.666	98.0
1023.4	.111	27.9	1008.3	.649	97.3
1022.4	.733	49.8	1007.6	.574	99.0
1020.8	1.36	96.7	1006.2	.455	100.0
1020.4	1.41	97.7	1005.5	.392	100.9
1019.4	1.39	96.8	1004.3	.436	92.2
1018.6	1.22	98.7	1004.0	.321	100.0
1017.8	1.18	97.8	1002.6	.334	93.9
1016.9	1.12	97.8	1001.9	.29	-----
1016.4	1.11	97.8	1000.7	.491	100.0
1016.0	1.08	97.8	1000.0	.796	93.4
1015.4	1.07	98.7	999.3	1.25	94.9
1014.2	.981	97.9	999.8	1.62	94.9
1013.5	.967	97.9	998.2	2.05	96.1
1013.0	.938	98.9	997.6	2.82	98.2
1012.3	.888	97.9	996.6	3.50	95.9
1011.5	.831	97.0	996.1	3.89	96.1
1011.0	.752	97.9	995.2	4.10	96.1
1010.5	.816	95.0	994.8	4.05	95.9
1010.0	.760	96.0	994.2	3.99	98.0

λ in A	k in $10^3 cm^{-1}$	Yield in %	λ in A	k in $10^3 cm^{-1}$	Yield in %
993.3	3.71	97.6	977.9	1.24	101.0
992.9	3.42	94.9	977.3	1.07	102.1
991.7	3.18	98.0	976.7	1.17	99.2
991.2	3.15	98.1	976.2	1.11	100.0
990.6	2.89	98.2	974.8	.965	102.4
989.6	2.71	98.6	974.6	.910	103.2
989.3	2.62	96.6	974.1	.858	102.0
988.5	2.49	99.6	973.4	.762	103.3
987.9	2.25	96.2	972.5	.601	104.8
986.9	2.28	97.7	972.0	.512	101.1
986.3	4.20	94.2	971.0	.364	95.2
985.8	3.33	93.3	970.4	.29	98.3
985.2	2.15	97.6	969.2	.459	99.9
984.6	2.03	99.9	968.3	1.31	96.2
983.8	1.92	100.2	967.6	3.06	100.6
983.3	1.86	99.6	967.3	3.68	95.1
982.6	1.77	97.9	966.0	4.12	99.4
982.1	1.55	99.6	965.4	3.63	98.4
981.3	1.58	99.3	964.8	3.33	100.6
980.5	1.63	98.9	964.1	2.79	101.5
980.1	1.50	99.9	963.7	2.58	101.0
979.2	1.30	102.9	962.8	2.29	95.3
978.5	1.35	100.9	961.7	2.19	100.4

λ in A	k in $10^3 cm^{-1}$	Yield in %	λ in A	k in $10^3 cm^{-1}$	Yield in %
960.7	1.81	102.2	941.6	1.66	101.7
960.0	1.72	101.8	941.1	1.30	100.2
959.5	1.59	103.5	940.3	.852	101.5
958.4	1.36	104.0	939.3	.522	96.8
957.8	1.25	101.3	938.8	3.59	99.1
956.9	.953	105.8	937.9	2.16	103.4
956.7	.806	97.9	936.9	1.39	99.9
954.8	.486	98.5	936.1	.622	103.3
953.6	.297	111.4	934.5	2.08	104.5
952.3	3.75	103.9	933.8	1.27	103.1
951.3	3.21	101.9	933.3	.459	103.4
950.9	2.76	103.4	932.5	2.58	96.8
949.7	2.19	103.8	932.1	1.80	99.1
949.1	1.76	105.0	931.4	.684	102.0
948.1	1.58	104.9	931.0	3.44	96.8
947.4	1.27	-----	930.0	.675	99.6
946.7	1.04	100.1	928.8	.447	106.2
946.0	.690	102.1	927.8	.523	87.7
945.2	.288	103.7	927.3	1.25	101.4
944.5	1.17	94.6	926.8	.980	92.5
943.8	3.42	96.4	926.0	1.28	87.9
943.3	2.94	101.8	925.4	1.28	84.4
942.2	2.01	102.0	925.1	.623	89.4

λ in A	k in $10^3 cm^{-1}$	Yield in %	λ in A	k in $10^3 cm^{-1}$	Yield in %
924.7	1.37	92.2	906.7	2.22	103.4
924.0	1.76	93.6	905.8	1.82	99.0
923.5	.927	103.4	905.5	1.93	102.2
923.2	1.51	104.4	904.6	1.72	98.9
922.5	1.81	102.2	904.1	1.97	102.7
922.2	1.86	102.7	903.6	2.04	100.1
921.5	1.78	103.1	902.8	1.96	100.8
920.1	1.53	102.3	901.7	1.89	103.1
919.1	1.82	104.3	900.7	1.91	102.3
918.7	1.84	104.0	900.2	2.05	104.3
917.8	1.79	101.8	899.6	2.08	105.6
917.0	1.85	103.6	898.6	1.76	96.5
916.0	1.85	103.1	898.2	1.86	104.2
914.8	1.95	102.5	897.1	2.00	102.3
914.2	1.92	102.7	896.2	2.04	103.2
913.5	1.98	102.8	895.5	2.33	108.6
912.2	1.95	103.3	894.6	1.96	102.2
911.5	1.95	103.5	893.4	1.93	102.5
910.6	1.92	103.5	892.4	1.94	102.2
909.6	1.94	104.0	891.2	1.89	102.8
908.6	2.07	100.2	890.3	1.95	106.8
908.1	1.98	99.8	889.7	1.93	99.2
907.7	1.95	101.6	889.0	1.90	101.4

λ in A	k in $10^3 cm^{-1}$	Yield in %	λ in A	k in $10^3 cm^{-1}$	Yield in %
888.1	1.88	102.6	871.7	1.86	88.9
887.7	1.86	100.7	871.4	1.81	88.2
887.2	2.02	101.7	869.9	1.82	81.2
886.5	1.86	100.6	869.7	1.81	104.3
885.8	1.90	100.0	868.5	1.93	96.9
885.0	1.95	100.6	867.9	----	-----
884.1	1.93	101.8	867.4	1.81	109.6
883.5	1.81	100.8	866.9	1.99	96.9
882.5	1.97	100.6	866.0	1.86	108.6
882.1	2.00	99.3	865.6	1.84	97.6
881.7	2.06	98.1	865.1	1.71	105.1
881.0	1.83	99.1	864.7	1.87	108.0
880.1	1.87	102.4	864.3	1.80	101.8
879.6	1.85	100.6	863.4	1.77	101.2
878.9	1.88	-----	862.6	1.78	106.3
877.4	1.89	102.3	862.1	1.79	102.9
876.5	2.00	94.1	860.3	1.81	96.1
875.8	1.95	92.4	859.8	1.75	96.8
875.1	1.58	99.0	859.5	1.78	96.0
874.3	1.93	95.7	857.9	1.61	114.6
873.6	1.90	99.9	857.6	1.80	111.7
872.9	1.98	103.7	857.0	1.80	115.3
872.1	1.98	104.0	855.7	1.78	104.6

λ in A	k in $10^3 cm^{-1}$	Yield in %	λ in A	k in $10^3 cm^{-1}$	Yield in %
855.3	1.77	106.0	852.2	1.75	-----
854.1	1.76	96.1	851.5	1.73	-----
853.2	1.69	-----	850.6	1.73	-----
852.8	1.68	-----	850.2	1.84	-----